applied sciences

MDPI

Article

Energy Management of Virtual Power Plant Considering Distributed Generation Sizing and Pricing

Masoud Maanavi [1], Arsalan Najafi [2,*], Radu Godina [3], Mehrdad Mahmoudian [4] and Eduardo M. G. Rodrigues [5]

1 Faculty of Engineering, Sepidan Branch, Islamic Azad University, Sepidan 73611, Iran
2 Young Researchers and Elite Club, Sepidan Branch, Islamic Azad University, Sepidan 73611, Iran
3 UNIDEMI, Department of Mechanical and Industrial Engineering, Faculty of Science and Technology (FCT), Universidade NOVA de Lisboa, 2829-516 Caparica, Portugal
4 Firouzabad Institute of Higher Education, Firouzabad 74711, Iran
5 Management and Production Technologies of Northern Aveiro—ESAN, Estrada do Cercal 449, Santiago de Riba-Ul, 3720-509 Oliveira de Azeméis, Portugal
* Correspondence: arsalan.najafi@iausepidan.ac.ir

Received: 12 May 2019; Accepted: 10 July 2019; Published: 15 July 2019

Abstract: The energy management of virtual power plants faces some fundamental challenges that make it complicated compared to conventional power plants, such as uncertainty in production, consumption, energy price, and availability of network components. Continuous monitoring and scaling of network gain status, using smart grids provides valuable instantaneous information about network conditions such as production, consumption, power lines, and network availability. Therefore, by creating a bidirectional communication between the energy management system and the grid users such as producers or energy applicants, it will afford a suitable platform to develop more efficient vector of the virtual power plant. The paper is treated with optimal sizing of DG units and the price of their electricity sales to achieve security issues and other technical considerations in the system. The ultimate goal in this study to determine the active demand power required to increase system loading capability and to withstand disturbances. The effect of different types of DG units in simulations is considered and then the efficiency of each equipment such as converters, wind turbines, electrolyzers, etc., is achieved to minimize the total operation cost and losses, improve voltage profiles, and address other security issues and reliability. The simulations are done in three cases and compared with HOMER software to validate the ability of proposed model.

Keywords: virtual power plant; operation; sizing; smart grid

1. Introduction

For the first time, the concept of virtual power plant was presented in 1994, with the aims of distributed energy resources (DERs) observation, providing suitable interface for local components, activation of distributed control strategies, and optimal use of available capacity. In the distributed generation (DG) units, the load response and energy storage systems (ESSs) which are used as the unit entity, are called the 'virtual power plant' (VPP). According to the advantages of distributed generation resources and ESSs, a VPP can be an appropriate alternative for conventional fossil fuels. The need for modifying, changing, and displacing of energy consumption provides an efficient atmosphere to implement the VPPs [1,2]. Therefore, a VPP can be defined as a cluster of dispersed generating units, flexible loads, and storage systems that are grouped in order to operate as a single entity. The generating units in the VPP can employ both fossil and renewable energy sources.

Energy management is a common and widely spread concept, including all measures that are planned and implemented to ensure the minimum amount of energy consumed in different activities. Trading, industries, and organizations have found themselves under high economic and environmental pressure in the last two decades to minimize their consumptions. Economic competition in the world market (especially the electricity market) and increasing the state of environmental regulations and standards in order to reduce climate pollutants are the most important factors in investment costs and exploitation of all organizations [3]. Actually, energy management is an important instrument in assisting various institutions to reduce their costs in order to meet these essential goals to survive and succeed in long term. The energy management of the VPPs faces challenges that make it complicated. These challenges include uncertainty in production, consumption, energy prices, and availability of network components. The smart grid increases the ability of the energy management system in the fields of overcoming uncertainties, aggregation of renewable sources, load responsiveness, monitoring, and network control [4,5].

In [6], a pricing model for the electricity market of the previous day and the regulated market are proposed to maximize the expected profits of the VPP utilization, while the pricing problem is modeled as a two-stage stochastic program. In [7], a two-stage refinement optimization strategy has been proposed for pricing the VPP in day ahead and real time. The practicality of the decisions made and the operation of intelligent network infrastructure to overcome uncertainties are prominent features of this approach. With regard to the definition of a VPP, the energy management can be divided into two categories: smart home power management and smart grid energy management. Most of the work done in the field of smart home energy management has focused on the concept of load responsiveness in energy management to provide a timetable for the use of tools inside the building [8–11]. In the area of smart grids, due to the influence of DERs, the use of ESSs and responsive loads has been considered in order to manage the variable nature of renewable energy sources (RESs). In [12], an intelligent house energy management model is presented using integrated integer linear programming (LP) to reduce costs and pollution, which can be used in the real-time planning framework, components of a smart home including smart devices, storage systems, and distributed generations. In [13], home-consumer planning has a photovoltaic system without using a storage system under different pricing policies. An algorithm for energy management has been formulated based on linear programming approach in which the solar source uncertainty is modeled with respect to the forecasting points. In [14], the problem of the voltage profile optimization in a distribution system including distributed energy resources has been investigated. In [15], a mathematical model of complex integer linear programming is proposed to minimize the cost of smart home power. This home has a controlled and equipped storage and renewable resource. Linear approaches like linear programming (LP) category for steady-state analysis of distribution systems are getting more and more imperative due to the penetration of DERs [16]. A mixed integer linear programming (MILP) based approach for determining optimal number, type, and location of automation devices such as remotely controlled circuit breakers/reclosers, sectionalizing switches, remotely supervised fault passage indicators, has been presented in [17].

According to the concept of responsive loads, a smart grid, including responsive loads, DERs, batteries, and electric vehicles, is presented in [18]. Congestions in the lines are eliminated using the load shifting. Uncertainties in the price of electrical energy and the amount of new energy sources are demonstrated by a limited number of scenarios. The issue of energy management is modeled by mixed integer linear programming method. The impact of using the smart grid on the energy management system has been reviewed in [19]. In [20,21], a linear programming problem for energy management of multi-carrier energy systems has been presented.

Utilizing intelligent network technology will help to manage the operation cost and reliability. This can result in minimum daily energy consumption, increasing the hourly limit and reducing the amount of energy consumed. The uncertainty in the price of electrical energy is exhibited by a robust optimization method in [22,23]. With the development of the model presented in [19], the new energy management system for a VPP is extracted. The plant includes a set of responsive

loads, distributed discharges equipment, wind farms, and storage systems connected through a grid. Uncertainties in the price of electrical energy and the production of wind farms have been solved by robust optimization. Linear programming and direct optimal load flow have been used to implement the energy management algorithm.

In [24], the impact of forecasting accuracy and technical constraints on the energy management of VPP with and without the presence of smart grid has been investigated. The constraints of the storage system, stochastic generation of distributed resources, energy transfer constraints, and responsive loads are considered in this model. In order to model the uncertainties in electrical energy prices and generation of solar stations, point prediction method has been used [25]. In this study, the possibility of contingencies in power management of the VPPs has not been discussed.

In this paper, the contributions are listed as below:

- In this manuscript, with the development of the VPP model, an optimal formulation is proposed to manage the VPPs energy scheduling.
- The point prediction method is used to model non-deterministic variables with uncertainties and PSO methodology is proposed to solve the energy management concerns.
- Taking into account that the possibility of contingency occurrence and equipping the microgrid with the necessary instruments to monitor the situation quickly, the impact of those phenomena in a smart microgrid is investigated on the management process.
- Proposing a deterministic model for VPP energy management to monitor the contingencies of microgrid.
- The sizing and siting of VPP components are investigated under different scenarios with reliability evaluation.

2. Concept of Energy Management Problem

The VPPs consist of a set of DGs and responsive loads in a microgrid equipped with smart grid technology. Responsive loads as energy applicants, such as an industrial estate, colleges of a university, or a residential area can change their energy consumption in response to change in energy prices. The energy supply unit is responsible for energy management and can provide the energy required by the main grid and solar stations as a source of uncertain DGs. Beside each of the solar stations, there is an energy storage system that enables the energy management system to store or produce energy at appropriate times. The set of responsive loads, DERs and storage systems in the form of VPP, have the ability to buy energy from the main grid during low-cost energy hours and sell them at expensive periods [26,27]. It is assumed that the VPP does not play a role in determining market price. Energy management system is related to wholesale electricity market and energy price announced by the main network, is considered as market price. The VPP owns solar stations and does not pay for solar energy.

Using smart grid technology, there is a bidirectional relation between time and reality of energy management and users in the microgrid. The energy management system will receive information about energy suppliers, including the energy price and the availability of obtainable power several minutes before the energy delivery date. Based on this information, the energy management system determines the optimal consumption rate, storage, and energy exchange for each time period and subsequent periods to send decisions a few minutes before the deadline for energy delivery to applicants and energy suppliers. These decisions are made in such that the social welfare of the VPP will include the difference in the cost of energy supply from the income of the applicants. Notice that information about the availability of network components including production resources and transmission lines is provided to the energy management system according to the scheduling period. If anything else happens, the energy management system will modify the decisions taken in the previous step to distribute power. The microgrid is also assumed to run at the beginning of the planning period.

3. Mathematical Formulation

Figure 1 shows the proposed microgrid structure that interacts with the electricity market. As shown in this figure, the considered system includes wind turbine units, solar cells, electrolytic reservoirs, hydrogen fuel storage tanks, fuel cells, batteries, and Direct current (DC)/Alternative current (AC) converters and loads (in the proposed model, the load types are considered as non-interruptible). In an autonomous microgrid, distributed energy sources should be able to balance their production and consumption with sufficient capacity and proper operation, while islanded from the upstream network. In the proposed model of this paper, resources will only sell energy on the day-ahead market to the upstream distribution network due to the compatibility with the objective function target (cost minimization/profit maximization).

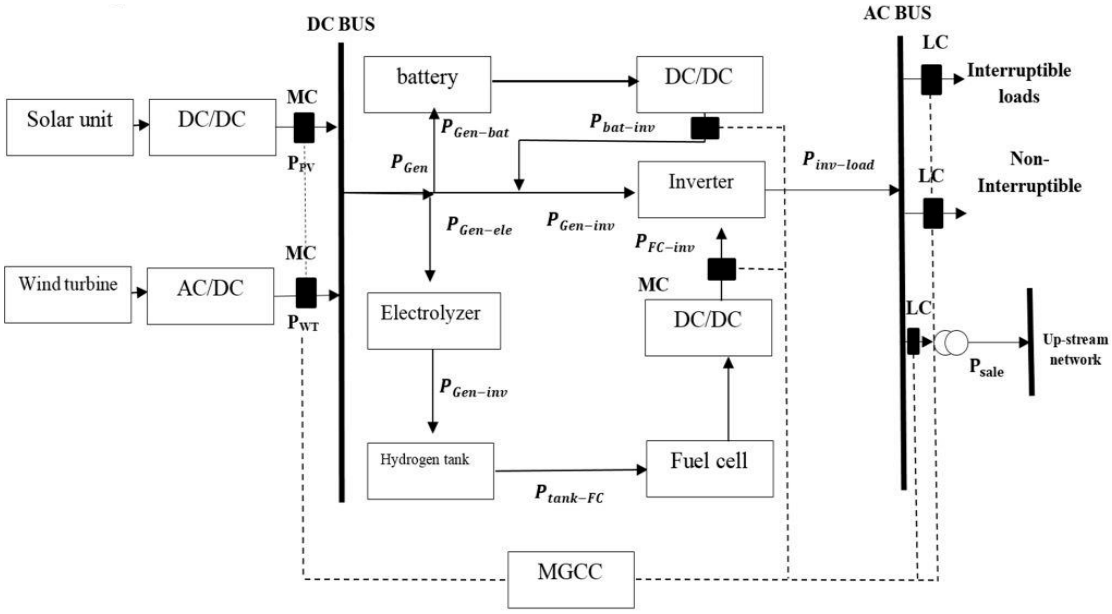

Figure 1. Centralized control micro-grid (MGCC) structure with the electricity market interaction.

Where in the above figure we have:

- P_{PV}: Output power of each solar unit (kW)
- P_{WT}: Output power of each wind turbine (kW)
- P_{Gen}: Total power generated by renewable energy units (kW)
- $P_{Gen\text{-}ele}$: Transmission power from renewable sources to electrolyzer (kW)
- $P_{Gen\text{-}bat}$: Transmission power from renewable sources to battery (kW)
- $P_{Gen\text{-}inv}$: Transmission power from renewable sources and battery to DC/AC converter (kW)
- $P_{ele\text{-}Tank}$: Transmission power from electrolyzer to hydrogen tank (kW)
- $P_{bat\text{-}inv}$: Transmission power from battery to DC/AC converter (kW)
- $P_{tank\text{-}FC}$: Transmission power from hydrogen tank to fuel cell (kW)
- $P_{FC\text{-}inv}$: Transmission power from fuel cell to DC/AC converter (kW)
- $P_{inv\text{-}load}$: Transmission power from DC/AC converter to load and upstream network (kW)
- P_{sale}: Wholesale power sold to up-stream network (kW)

3.1. Solar Unit

The data received from the sun to the array surface is converted to its output power using the equation

$$P_{PV} = {}^{G}/_{1000} \times P_{PV,rated} \times \eta_{pv,conv} \quad (1)$$

In Equation (1), G is the radiation power perpendicular to the array surface (W/m^2) and $P_{PV,rated}$ represents the nominal power of each array, which is obtained for the cost. $\eta_{PV,conv}$ is also equivalent to the efficiency of the DC/DC converter installed between each DC array and the corresponding bus. By verifying the vertical and horizontal component of the solar power, at any moment, the power can be transmitted (vertically) onto the surface of the array installed with the angle θ_{PV} could be calculated according to (2)

$$G(t, \theta_{PV}) = G_V(t) \times \cos(\theta_{PV}) + G_H(t) \times \sin(\theta_{PV}) \quad (2)$$

where $G_H(t)$ and $G_V(t)$ are the horizontal and vertical radiation rates in terms of (W/m^2), respectively.

3.2. Wind Turbine Unit

The wind turbine class used in this paper is BWC Excel-R/48. Output power (P_{WT}) in terms of wind speed (v_W) can be approximated by relation (3) [17]

$$P_{WT} = \begin{cases} 0 & ; v_w \le v_{cutin}, v_w \ge v_{cutout} \\ P_{WT\max} \times \left(\frac{v_w - v_{cutin}}{v_{rated} - v_{cutin}}\right)^m & ; v_{cutin} \le v_w \le v_{rated} \\ P_{WT\max} + \frac{P_{furl} - P_{WT\max}}{v_{cutout} - v_{rated}} \times (v_W - v_{rated}) & ; v_{rated} \le v_w \le v_{cutout} \end{cases} \quad (3)$$

where v_{cutin}, v_{cutout}, and v_{rated} are the cut-off wind speed, the high cut-off rate and the nominal speed (m/s) of the turbine, respectively. The parameter $P_{WT,\max}$, shows the maximum turbine output power (kW) and P_{furl}, also have an output power at the high cut-off speed. In this paper, m is considered to be (3).

3.3. Electrolyzer Unit

The function of electrolyzer, is decomposition of water into hydrogen and oxygen by a simple electrolysis process. In this way, the direct current of electricity passes through the path between two electrodes that immersed in water, causing water to decompose into oxygen and hydrogen. Oxygen is produced in the cathode and hydrogen at the anode side. In the proposed model, this paper is used to reduce the energy consumption of a compressor-less design, due to the usage of a polymer electrolyte membrane (PEM) fuel cell. In view of the fact that in this type of pressure fluid, the pressure required by hydrogen is 1.2 bar, the developed is very flexible and can be easily added to the compressor model. The electrochemical interactions in the electrolysis apparatus of water are

$$H_2O \rightarrow \frac{1}{2}O_2 + 2H^+ + 2e^- \quad (4)$$

To model the electrolyzer, its efficiency is used as an input parameter. The thermal value of hydrogen is 3.4 kV per cubic meter, which, taking into account the efficiency of 90% for an electrolyzer to produce a kilogram of hydrogen, consumes energy at 41.99 kWh/kg as (5).

$$Consumed\_Power = \frac{\frac{3.4(\text{kwh/m}^3)}{0.09(\text{kg/m}^3)}}{90} \times 100 = 41.97\text{kwh/kg} \quad (5)$$

The hydrogen weight produced by the excess of energy produced from the system to the electrolyzeris obtained at 41.97 kWh/kg.

$$Generated\_H_2 = \frac{P_{\text{electrolyzer}}(\text{kwh})}{41.97(\text{kwh/kg})} \quad (6)$$

3.4. Fuel Cell Unit

PEMs have a relatively fast dynamic response, about 1 to 3 s. The power output of these fuel cells can be calculated as a function of the input power of the hydrogen as well as its efficiency (η_{FC}), which can be assumed to be constant. Therefore the output power extracted from fuel cell stacks ($P_{FC\text{-}inv}$) could be represented with (7) in which $P_{tank\text{-}FC}$ is gross productive power of fuel cells.

$$P_{FC\text{-}inv} = P_{tank\text{-}FC} \times \eta_{FC} \tag{7}$$

3.5. Hydrogen Tank Unit

The energy stored in the tank for each step t, can be calculated as

$$E_{\tan k}(t) = E_{\tan k}(t-1) + P_{el\text{-}\tan k} \times \Delta t - (P_{\tan k\text{-}FC}(t) \times \Delta t)/\eta_{storage} \tag{8}$$

where, Δt is the length of each time step, P_{el_tank}, represents the transmission power from the electrolyzer to the hydrogen tank and P_{tank_FC}, can be transmitted from the hydrogen tank to the fuel cell. The term $\eta_{storage}$ also signifies the efficiency of the storage system, which can indicate losses due to leakage or pumping. However, the hydrogen in the tank will always have a high and low range limitations, as

$$E_{tank,\min} \le E_{tank}(t) \le E_{tank,\max} \tag{9}$$

3.6. Energy Storage (Battery) Unit

The battery source is used to provide the load in the absence of renewable energy sources. The difference between the power produced and the load power required indicates whether the battery should be charged or discharged. The amount of charge of the battery bank is obtained in time horizon t using the following Equation (10)

$$E_{bat}(t) = E_{bat}(t-1) + P_{Gen\_bat} \times \Delta t \times \eta_{bat} - (P_{bat\_inv}(t) \times \Delta t)/\eta_{dis\_bat} \tag{10}$$

where, E_{bat} (t) represents the amount of battery electric energy at time t. By the way, η_{bat} and η_{dis_bat}, are the charge and discharge efficiency of the battery bank, respectively.

4. Reliability

There are several references which have provided several indicators for calculating the reliability of systems, including indicators such as loss of load expectation (*LOLE*), loss of energy expectation (*LOEE*), or expected energy not supplied (*EENS*), loss of power supply probability (*LPSP*), equivalent loss factor (*ELF*), and so on. The above indicators are defined by the following relationships. In this paper, Markov chain method is used to calculate the reliability parameters. Other required parameters are also derived from [28–30].

$$LOLE = \sum_{t=1}^{N} E[LOL(t)] \tag{11}$$

In the above relation, $E[LOL(t)]$ is the mathematical expectation of the time offset in time t, which can be defined by

$$E[LOL] = \sum_{s \in S} T_s \times P_s \tag{12}$$

In this case, P_s is the probability of being in the state of s and T_s in the case of being in this situation. S is the total set of possible situations for the system. Therefore

$$LOEE = EENS = \sum_{t=1}^{N} E[LOE(t)] \tag{13}$$

Here $E[LOE(t)]$ is the mathematical expectation of the amount of lost energy in the time interval t that can be defined by

$$E[LOE] = \sum_{s \in S} Q_s \times P_s \tag{14}$$

Q_s is the amount of lost load (kWh) if positioned in s. The probability of loss of source (LPSP) is obtained according to (15).

$$LPSP = \frac{LOEE}{\sum_{t=1}^{N} D(t)} \tag{15}$$

In the above relation, it is assumed that $D(t)$ is equal to the load demand (kWh) in time t. Finally, the equivalent load offset coefficient can be defined as (16)

$$ELF = \frac{1}{N} \sum_{t=1}^{N} \frac{Q(t)}{D(t)} \tag{16}$$

Since the *ELF* contains more information, both the number of determinations N (and the values of $Q(t)$), this paper is used as the main criterion of reliability. The maximum allowed for *ELF* in developed countries is equal to 0.0001, however, for an independent system to the network, this limit is considered to be 0.01.

5. Objective Function

Life cycle cost analysis evaluates the costs of covering all expenditures incurred during the activity period. The net present cost (NPC) is used as the charge of the system life cycle. The NPC includes initial installation costs, replacement costs, repairs, and maintenance of the equipment, the cost of the power failure, the cost of connecting to the grid. In NPC calculations, the costs are considered positive and earnings are considered negative.

All costs and expenses are assessed at a fixed interest rate throughout the year. In this type of assessment, in order to influence the increase rate in calculations at the end of the process of analysis and review of the system, it should be applied to the NPC, by calculating the real interest rate caused by inflation, according to certain relationships. The real interest rate is the difference between the nominal interest rate and the inflation rate. The NPC value of the equipment can be calculated according to the equation

$$NPC_i = N_i \times (CC_i + RC_i \times K_i + O\&MC_i \times PWA(ir, R)) \tag{17}$$

In the above statement, N will equip the unit, or capacity (kW or kg), CC is initial investment cost ($/unit), RC stands for cost of each replacement annual maintenance cost ($/unit-year) equipping at R project lifetime (in this study is 20 years). The cost of the initial purchase of hydrogen is considered at the cost of the tank investment and represents real interest, which can be calculated in terms of the nominal interest ($ir_{nominal}$) and the annual inflation rate (ir) in accordance with Equation (18).

$$ir = \frac{(ir_{nominal} - f)}{(1 + f)} \tag{18}$$

PWA and *K* are respectively the annual and constant payments current value, which are defined as

$$PWA(ir, R) = \frac{(1+ir)^R - 1}{ir(1+ir)^R} \tag{19}$$

$$K_i = \sum_{n=1}^{y_i} \frac{1}{(1+ir)^{n \times L_i}} \tag{20}$$

y and *L* are the number of replacements and useful life of the equipment, respectively. For each component of the system, the initial cost, in accordance with the cost in year zero, is the replacement cost according to the need to replace that component at the end of its lifetime and the cost of *O* & *MC* for each year of the project. The cost of replacing a component varies for several reasons with its initial cost. One of these reasons is that when replacing a component due to the expiration of its life-span, all the components of that component that have been expended during the initial installation do not need to be replaced.

5.1. Interruption Power Cost

The interruption cost of electricity equals the cost of damages caused by power outages to consumers. The cost of interrupting the supply of electrical energy required by load is estimated by different methods. For example, this can be calculated based on the willingness of the customer to pay for the expansion of the network or the losses incurred by the industries due to the interruption created in their production process. If the amount of lost hope is defined annually with relation (21),

$$LOEE = EENS = \sum_{t=1}^{N} E[LOE(t)] \tag{21}$$

Then, the net present value of the load loss can be obtained according to (22)

$$NPC_{loss} = LOEE \times C_{loss} \times PWA \tag{22}$$

In fact, the Equation (22), is equal to the average loss due to the disconnection of every kW hour of charge ($/kWh). Regarding the type of load (non-removable, etc.) mentioned previously, the average loss due to the interruption of each kWh is different.

5.2. Power Sailing Revenue

Since the goal is to minimize the operation costs of objective function, we introduce negative revenue from the sale of electricity to the upstream network in the calculations. The net present value of electricity sales to the upstream network is

$$NPC_{sale} = \sum_{t=1}^{8760} \left(P_{sale}(t) \times C_{sale}(t) \times PWA(ir, R)\right) \tag{23}$$

In the above-mentioned equation, C_{sale} is the revenues generated by selling electricity power in (kW/hour) to the upstream network, while it depends on the time of the power exchange and the price of energy at that period. Given the costs and income mentioned above, the objective function is defined as (24).

$$J = \min_x \left\{ \sum_i NPC_i + NPC_{loss} + NPC_{miss} + NPC_{T\&D} - NPC_{sale} \right\} \tag{24}$$

where *i* represents the desired equipment and *x* is a vector of optimization variables.

5.3. Constraints

At any given interval, the total production capacity of the hybrid production system should be able to meet the total demand for the load, taking into account the terms and conditions of reliability, which is calculated by the equation

$$P_{Gen\_inv}(t) + P_{FC\text{-}inv}(t) = (P_{Load}(t) + P_{sale}(t))/\eta_{inv} \tag{25}$$

Accordingly, $P_{Load}(t)$, $P_{sale}(t)$, $P_{Gen\_inv}(t)$, $P_{FC\_inv}(t)$ represent the total load demand (disconnect-able and non-interruptible), high power upstream network, the power transmitted from DGs to battery and the transient power from fuel cell stacks to the DC/AC converter, respectively. Since 10% of the total demand per hour is considered as a removable load and the remaining 90% is assumed as an irremovable load, Therefore, when ($Loss\_power$ $(t)/P_{Load}$ $(t) < 0.1$), load interruptions are not included in the reliability calculations of the system. Consequently, when ($Loss\_power$ $(t)/P_{Load}$ $(t) > 0.1$), the ELF index in the reliability calculations of the system is computed. Thus, until the Equation (33) is correct, the load procurement can be continued.

$$E[ELF] \leq ELF_{max} \tag{26}$$

and the capacity to be sold to the upstream network should not exceed a certain limit, which is determined by prior agreements

$$P_{sale} \leq P_{sale}^{\max} \tag{27}$$

The energy stored in the hydrogen tank and the battery should be within the following limits:

$$E_{batmin}(t) \leq E_{bat}(t) \leq E_{bat\text{-}Max}(t) \tag{28}$$

$$0 \leq E_{tank}(t) \leq E_{tank\text{-}Max}(t) \tag{29}$$

$$E_{bat}(0) \leq E_{bat}(8760) \tag{30}$$

$$E_{tank}(0) \leq E_{tank}(8760) \tag{31}$$

The last two constraints imply that the energy stored in the tank and the battery at the end of the year should not be less than the energy stored at the beginning of the year. This ensures that the reliability calculations are performed for the worst possible situation.

The proposed formulation is optimized using particle swarm optimization (PSO) algorithm. The capacity of DGs is constant while the number of DGs is variable. In the other words our variables should be optimized are the number of DGs using PSO. By optimizing the variable, the objective function is concluded which is the total cost of VPP. The interested readers are referred to [31] for more studying about PSO.

5.4. Optimization Algorithm

Particle swarm optimization is an evolutionary and population-based algorithm that presented introduced by Eberhart and Kennedy [32]. Each particle in PSO is a candidate solution in search space of the problem. There are two main parts in these candidate solutions—current position (X_i) and current velocity (V_i)—described as

$$\begin{aligned} X_i(k) &= \left(x_i^1(k), x_i^2(k), ..., x_i^n(k)\right) \\ V_i(k) &= \left(v_i^1(k), v_i^2(k), ..., v_i^n(k)\right) \end{aligned} \tag{32}$$

where n is the dimension of problem (solution) and k is the iteration index. New position of each particle is updated using current position and new velocity. New velocity also is produced by four

factors including: current velocity, current position, best previous position of particle (*Pbest*), and best position in all particles of all iterations (*GBest*). Then, the new velocity is represented as

$$v_{i,j} = \omega v_{i,j} + c_1 r_1(\cdot)\left[pbest_{i,j} - x_{i,j}\right] + c_2 r_2(\cdot)\left[gbest_j - x_{i,j}\right] \quad (33)$$

where ω is particle inertia coefficient, c_1 and c_2 are accelerations coefficient, respectively. r_1 and r_2 are uniform random numbers between 0 and 1. New positions are obtained as

$$x_{i,j} = x_{i,j} + v_{i,j} \quad (34)$$

where $pbest_{i,j}$, is the particle best of position i with dimension j and $gbest_j$ is the dimension j of G_{best}. The PSO algorithm is depicted in Figure 2.

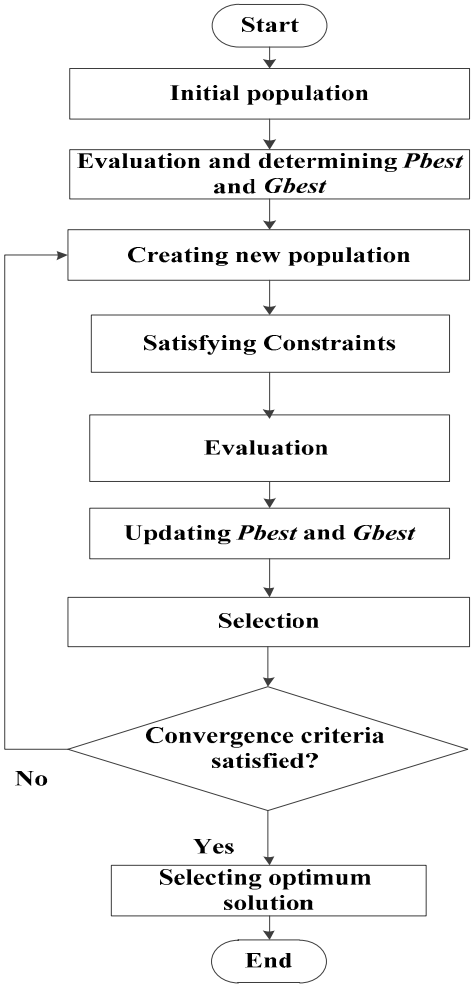

Figure 2. PSO algorithm flowchart.

6. Simulation Results and Discussion

The capacity of each wind turbine is considered as 7.5 kW, 1 kW for each solar array, power of each electrolyzer and fuel cell are measured to 1 kW, then the size of each hydrogen tank is 1 Kg and the amount of energy stored per battery is 9.6 kWh. Tables 1 and 2 contain the specifications of the system equipment, which are modeled. Also, the real interest rate (u) is 0.08 *ir*. Considering the useful life of the project is 20 years, the *PWA (ir, R)* value is 9.818.

Table 1. Specifications of the system equipment.

Equipment	Initial Cost (US$/unit)	Replacement Cost (US$/unit)	Annual Cost of Maintenance	Useful Life (Year)	Efficiency
Wind turbine	19,400	15,000	75	20	-
Solar array	7000	6000	20	20	-
Electrolyzer	2000	1500	25	20	75
Hydrogen tank	1300	1200	15	20	95
Fuel cell	3000	2500	175	5	50
DC/AC converter	800	750	8	15	90
Battery	12,500	1100	65	4	85

Table 2. Wind turbine specification.

Rated Power	Output Power	Output Power in High Interruption Speed	High Interruption Speed (m/s)	Rated Power (m/s)	Low Interruption Speed (m/s)
7.5	8.1	5.8	25	11	3

The maximum power available at upstream network is 500 kW. Also, the energy prices sold to the high-voltage network during different hours of the day are from the spring and autumn periods are those written in accordance with Table 3. The seasonal coefficient of summer and winter is defined as 1.3 and 0.8.

Table 3. Energy purchased price from upstream network.

Hour	Price (US$/kWh)	Hour	Price (US$/kWh)
1	0.1	13	0.15
2	0.1	14	0.15
3	0.1	15	0.15
4	0.1	16	0.15
5	0.1	17	0.15
6	0.1	18	0.3
7	0.1	19	0.3
8	0.1	20	0.3
9	0.15	21	0.3
10	0.15	22	0.3
11	0.15	23	0.1
12	0.15	24	0.1

The interruption cost for a removable load equivalent is 0.1 ($/kWh) and for non-removable loads equivalent is 0.5 ($/kWh). The price of electricity sales to domestic grid users (which is considered as the maximum profit for these prices) is at different times according to Table 4.

Transmission lines and transformer investment costs are 5% of equipment costs, as well as miscellaneous network costs. The cost cannot be evaluated precisely such as financial transaction fees, accounting costs, transportation, advertising and marketing, etc. Then there is 38% of the cost of installing scattered units and the cost of repairing and maintaining grid equipment, and 5% of the cost of repair and maintenance of dispersed production units. In this section, in order to validate the results of the developed software, initially, the results of the size and optimization of the three hybrid systems as shown in Figures 3–5. They are compared with the output results extracted from the HOMER software. Hybrid systems consist of solar panels, wind turbines, and energy storage systems. In the hybrid system number 1, the hydrogen tank, in system 2, the battery and in system number 3, the battery and hydrogen tank are used as an energy storage device.

Table 4. Selling electricity price to domestic microgrid end users.

Time	Price (US$/kWh) Interruptible Loads	Price (US$/kWh) Non-Interruptible Loads
1	0.1	0.5
2	0.1	0.5
3	0.1	0.5
4	0.1	0.5
5	0.1	0.5
6	0.1	0.5
7	0.1	0.5
8	0.1	0.5
9	0.1	0.5
10	0.1	0.5
11	0.1	0.5
12	0.1	0.5
13	0.1	0.5
14	0.1	0.5
15	0.1	0.5
16	0.1	0.5
17	0.1	0.5
18	0.1	0.5
19	0.1	0.7
20	0.1	0.7
21	0.1	0.7
22	0.1	0.7
23	0.1	0.5
24	0.1	0.5

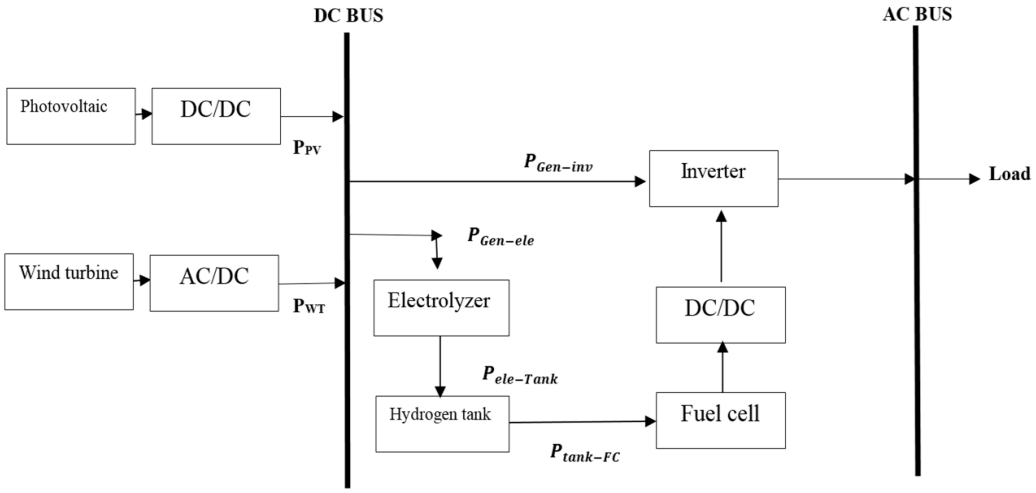

Figure 3. Hybrid system No. 1 (with hydrogen tank).

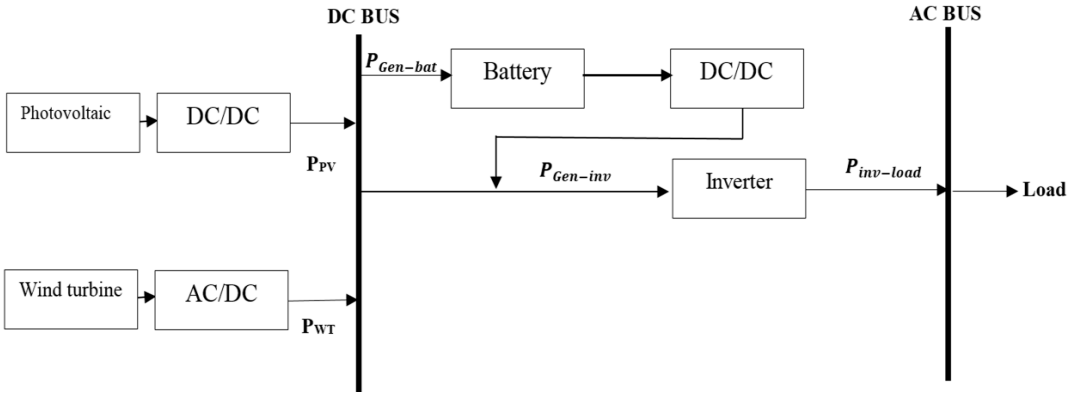

Figure 4. Hybrid system No.2 (with battery).

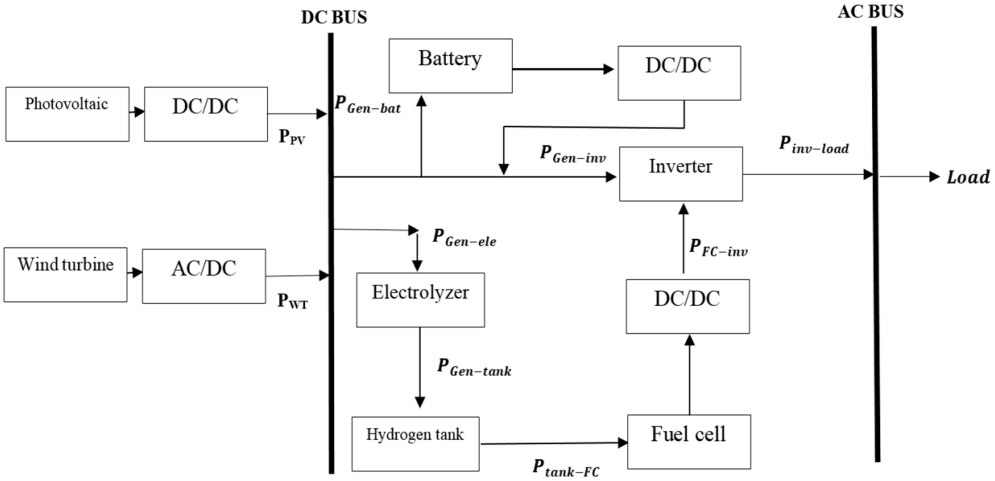

Figure 5. Hybrid system No. 3 (with both battery and hydrogen tank).

The results obtained from HOMER software are compared with the results obtained from the software developed in MATLAB environment, shown in Table 5.

Table 5. Numbersof DERs in three hybrid systems.

Case No.	Method	Number of Wind Turbine	Number of Solar Units	Number of Electrolyzer	Number of Hydrogen Tank	Number of Fuel Cell	Number of Battery	Cost (Dollar)
System No.1	PSO	111	2015	1192	829	515	——	2.53165
	HOMER	112	2015	1192	829	516	——	2.5328×10^7
System No.2	PSO	379	1623	——	——	——	7099	4.4235×10^7
	HOMER	380	1623	——	——	——	7099	4.4236×10^7
System No.3	PSO	768	634	1655	2010	543	8	2.6842×10^7
	HOMER	769	633	1654	2009	544	9	2.6896×10^7

According to Table 5, the results obtained by HOMER software are very close to the results obtained from the developed software and confirm the accuracy of the developed coding. Also, the results of the review of the three hybrid systems show that the use of battery as a storage device instead of an electrolyzer assembly, hydrogen tank, and fuel cell will increase system costs. Therefore, this price rising is justified by the high speed of the battery in pursuit of charge.

Table 6, also shows the optimal number of energy resources extended by considering the virtual power plant, the amount of revenue, and costs of the proposed grid.

Table 6. Optimal number of energy resource.

Number of Battery	Number of Fuel Cell	Number of Hydrogen Tank		Number of Electrolyzer	Number of Solar Units	Number of Wind Turbine
25	643	1631		2160	1367	227
Total cost ($)	Electricity revenue from sales to the Upstream Network ($)	Transmission and transformer lines cost ($)	Incidental costs ($)	Cost of electricity cut-off ($) (Interruptible and Non-Interruptible)	Value of lost load (kWh)	Sold power to upstream network (kWh)
1.852×10^7	9.860×10^6	1.282×10^6	1.45×10^4	3.19×10^5	4.590×10^5	9.860×10^6

Now, considering the uncertainty in wind energy, for the 95% confidence level, we solve the problem again with the result of optimization presented in Table 6. then, Figure 6 represents the total cost of the system in terms of the number of repeat steps.

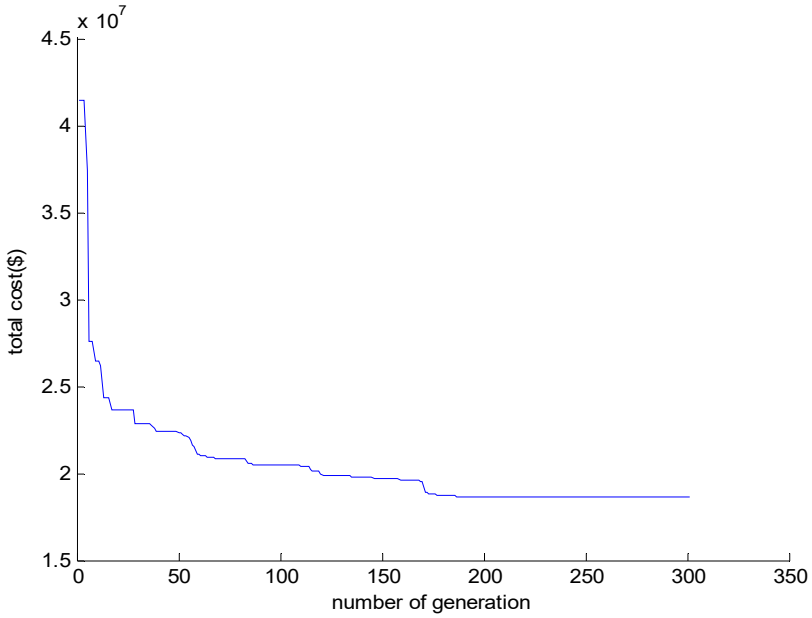

Figure 6. Total cost of system in terms of iteration.

Table 7 shows the optimal number of sources of energy, the amount of income and expenses of the proposed grid.

Table 7. Optimal number of energy resources considering uncertainty.

Number of Battery	Number of Fuel Cell	Number of Hydrogen Tank		Number of Electrolyzer	Number of Solar Units	Number of Wind Turbine
59	395	2179		1339	1850	126
Total cost ($)	Electricity revenue from sales to the Upstream Network ($)	Transmission and transformer lines cost ($)	Incidental costs ($)	Cost of electricity cut-off ($) (Interruptible and Non-Interruptible)	Value of lost load (kWh)	Sold power to upstream network (kWh)
1.975×10^7	8.234×10^6	1.313×10^6	$1.3.19 \times 10^4$	3.3443×10^5	3.514×10^5	8.234×10^6

The output results show that the inclusion of uncertainty in the output power of wind units increases the cost, and this growth in costs is justified by increasing the reliability level of wind turbine output, which increases the level of reliability in the output of wind turbines, correspondingly. The average reliability of the system will be reduced from 0.053 to 0.042 during the year, or increase the reliability of the system. Now we are examining and simulating system scenarios.

6.1. Cut-Off Wind Effect

In Table 8, the effect of cut-off wind turbine speed on the optimum size and cost of the proposed grid is shown.

Table 8. Effect of cut-off wind turbine speed on the optimum size and cost.

Low Cut-Off Speed of Wind Turbine (m/s)	1	3	5
Number of Wind Turbines	329	225	142
Number of Photovoltaic Units	939	1364	1774
Number of Electrolyzers	2017	2290	2673
Number of Hydrogen Tanks	1327	1635	1875
Number of Fuel Cells	313	370	396
Number of Batteries	23	27	46
Incidental Costs ($)	1.201×10^4	1.29×10^4	1.76×10^4
Transmission and Transformer Lines Cost($)	1.19×10^6	1.282×10^6	1.372×10^6
($)Cost of Electricity Cut-Off	3.43×10^5	5.17×10^5	6.92×10^5
Electricity Revenue from Sales to the Upstream Network ($)	8.821×10^6	9.472×10^6	1.141×10^7

As it can be seen, while the number of wind turbines with low cut-off speed is decreased, the total cost increases by growing the cut-off speed. This indicates that more wind turbines working with low cut-off speed means less power will be generated. Therefore, other DGs have to operate at a higher power level and this raises the cost of operation. It is because the input of wind turbines is cheap wind energy, while some of those DGs use hydrogen fuel or heat as input power.

6.2. PV Investment

In Table 9, the effect of initial investment cost of solar panels on the optimum size and cost of the system is presented.

Table 9. Effect of initial investment cost of solar panels on the optimum size and cost.

Initial Investment Cost of Solar Arrays ($/kw)	6000	7000	8000
Number of Wind Turbines	184	225	321
Number of Photovoltaics Units	1419	1364	1265
Number of Electrolyzers	2137	2290	3494
Number of Hydrogen Tanks	1554	1635	1948
Number of Fuel Cells	329	370	427
Number of Batteries	20	27	41
Incidental Costs ($)	1.03×10^4	1.29×10^4	1.411×10^4
Transmission and Transformer Lines Cost ($)	1.04×10^4	1.282×10^6	1.299×10^6
Cost of Electricity Cut-Off ($)	5.05×10^5	5.17×10^5	2.1009×10^5
Electricity Revenue from Sales to the Upstream Network ($)	1.009×10^7	9.472×10^6	8.753×10^6
Total Cost ($)	1.613×10^7	1.772×10^7	1.962×10^7

According to Table 9, as the investment costs increase, the number of solar units and prices decrease. This is because the cheap and common energy of the sun will be less used and should be directed towards other energies like wind. Since the capacity of wind resources is also limited, the utilization of costly resources is required, which results in increasing the costs of exploitation.

6.3. DC/AC Converter

In Table 10, the effect of the DC/AC converter efficiency on the optimal size and cost of system execution is shown.

Table 10. Effect of the DC/AC converter efficiency on the optimum size and cost.

Efficiency of DC/AC Converter (%)	70	90	100
Number of Wind Turbines	231	225	201
Number of Photovoltaics Units	1671	1364	201
Number of Electrolyzers	2314	2290	1561
Number of Hydrogen Tanks	1741	1635	1116
Number of Fuel Cells	432	370	310
Number of Batteries	33	27	21
Incidental Costs ($)	1.52×10^4	1.29×10^4	1.17×10^4
Transmission and Transformer Lines Cost ($)	1.419×10^6	1.282×10^6	1.1001×10^6
Cost of Electricity Cut-Off ($)	5.82×10^5	5.17×10^5	4.63×10^5
Electricity Revenue from Sales to the Upstream Network ($)	8.828×10^6	9.472×10^6	1.012×10^7
Total Cost ($)	1.9103×10^7	1.772×10^7	1.6117×10^7

According to Table 10, it is expected to decrease costs by increasing the efficiency of the converter. As the converter efficiency rises, the power losses are reduced, correspondingly. Then, with lower energy production, all demands will be supplied sufficiently.

6.4. Effect of Selling Electricity to the Upstream Network

In Table 11, the effect of the electricity exchanging price to the upstream network in non-peak hours is represented. This issue has been obtained in terms of the optimal size assessment of DGs considering grid connected operation mode.

Table 11. Effect of the electricity sales price on the optimum size and cost.

Electricity Sale Price to Upstream Network ($)	0.1	0.2	0.25
Number of Wind Turbines	225	183	132
Number of Photovoltaics Units	1364	2783	5132
Number of Electrolyzers	2290	3297	4519
Number of Hydrogen Tanks	1635	3542	4391
Number of Fuel Cells	370	430	541
Number of Batteries	27	53	64
Incidental Costs ($)	1.29×10^4	1.39×10^4	1.452×10^4
Transmission and Transformer Lines Cost ($)	1.282×10^6	1.371×10^6	1.51×10^6
Cost of Electricity Cut-Off ($)	5.17×10^5	5.87×10^4	5.98×10^3
Electricity Revenue from Sales to the Upstream Network ($)	9.472×10^6	1.108×10^7	1.838×10^7
Total Cost ($)	1.772×10^7	1.036×10^7	9.752×10^6

According to Table 11, the increase in electricity sales prices to the upstream network will increase the sales of electricity to the upstream network, which will reduce the total operation cost of system and it will raise the revenue.

6.5. Reliability Effects

In Table 12, the effect of increasing system reliability ($ELF(t)$ or reliability index reduction) has been shown on the optimum size and cost of performing grid.

Table 12. Effect of increasing system reliability on the optimum size and cost.

Amount of Reliability Index	0.1	0.05	0.01
Number of Wind Turbines	225	231	237
Number of Photovoltaics Units	1364	1692	2005
Number of Electrolyzers	2290	2381	2434
Number of Hydrogen Tanks	1635	831	344
Number of Fuel Cells	370	412	437
Number of Batteries	27	51	40
Incidental Costs ($)	1.29×10^4	1.302×10^8	1.38×10^4
Transmission and Transformer Lines Cost ($)	1.282×10^6	1.320×10^6	1.429×10^6
Cost of Electricity Cut-Off ($)	5.17×10^5	3.38×10^5	1.11×10^5
Electricity Revenue from Sales to the Upstream Network ($)	9.472×10^6	9.52×10^6	9.64×10^6
Total Cost ($)	1.772×10^7	1.91×10^7	2.12×10^6

According to Tables 13 and 14, increasing system reliability increases system costs, as expected.

As a total deduction in this paper, solar panels and wind turbines are used as power generators and from hydrogen batteries and tanks as energy storage. The proposed system consists of two types of loads which are interruptible loads such as little residential areas and non-interruptible loads like the hospitals. Then, the expression of the mathematical model of each of the components of the proposed micro-network energy system was presented. After expressing the model of the proposed grid elements and components, the objective function was proposed to minimize (maximize) 20-year costs of the system along with its constraints.

The proposed algorithm and some the state of art methods are applied on system No. 1, and compared as shown in Tables 13 and 14. The parameter considered for evaluation consists of total operation cost, expected energy not supplied (EENS), loss of power supply probability (LPSP), and the numbers of DGs crate the VPP. As it is observed, the proposed method has the lowest operation cost and the best reliability indices among other approaches.

Table 13. Different approach comparison.

Equipment	Operation Cost (US $)	EENS (%)	LPSP (%)
Genetic	2.934×10^7	17.4	12.1
TLBO	2.642×10^7	8.5	6.5
DE	2.799×10^7	13.2	11.6
SA	2.758×10^7	11.1	8.5
Proposed	2.531×10^7	5.6	2.5

Table 14. DG number obtained from different approaches.

Equipment	Genetic	TLBO	DE	SA	Proposed
Wind Turbine	131	122	202	167	111
Solar Array	2321	2109	2310	2380	2015
Electrolyzer	1255	1211	1212	1215	1192
Hydrogen Tank	955	922	952	942	829
Fuel Cell	629	555	644	641	515
Battery	32	4	35	36	—
Total	5323	4923	5355	5381	4662

7. Conclusions

From the studies made in this paper, the following results can be deduced:

- This major weakness greatly reduces the reliability of energy systems. The solution to this problem is the use of supportive production systems or energy storage systems, in which the battery and hydrogen tank are used as a storage system in order to provide optimal reliability.

- Compared to the use of storage systems, combining different energy sources that have complementary production characteristics (such as wind and sun) are considered as a convenient and inexpensive way to improve system reliability. The proposed grid has such a structure to overcome the above problems.
- Comparison of the results of determining the optimal capacity of the three hybrid systems suggests that using the battery as a storage device in a hybrid system instead of a fuel cell would increase system costs which increase the cost of the system by increasing the system's ability to track the load.
- The results show that simultaneous use of fuel and fuel cells as a storage medium in the hybrid system, in addition to reducing costs, also increases the system's ability to track the load. In addition, considering the disruptive load model as a virtual power plant reduces costs.
- The results of determining the size of resources distributed energy microgrid suggested that in view of the uncertainty in the power output of wind turbines increased costs (loss of income) of the system during its life, is that the increased cost (reduced revenue) is justified by increasing the level of reliability in the power output of wind turbines.
- Ability to cut off removable loads in case of necessity increases the reliability of the system and (possibly) reduces the cost of the grid.

Author Contributions: M.M. (Masoud Maanavi): writing and simulating original paper; A.N.: conceptualization, supervision, methodology and revising; R.G.: editing, data analyzing, funding acquisition; M.M. (Mehrdad Mahmoudian): Revising the paper; E.M.G.R.: editing.

Funding: Radu Godina would like to acknowledge financial support from Fundação para a Ciência e Tecnologia (UID/EMS/00667/2019).

Conflicts of Interest: The authors declare no conflict of interest.

References

1. Nakayama, K.; Chen, W.P. Aggregated and Optimized Virtual Power Plant Control. U.S. Patent Application US10103550B2, 18 August 2016.
2. Camal, S.; Michiorri, A.; Kariniotakis, G. Optimal offer of automatic frequency restoration reserve from a combined PV/wind virtual power plant. *IEEE Trans. Power Syst.* **2018**, *33*, 6155–6170. [CrossRef]
3. Pourghaderi, N.; Fotuhi-Firuzabad, M.; Moeini-Aghtaie, M.; Kabirifar, M. Commercial demand response programs in bidding of a technical virtual power plant. *IEEE Trans. Ind. Inf.* **2018**, *14*, 5100–5111. [CrossRef]
4. Moutis, P.; Georgilakis, P.S.; Hatziargyriou, N.D. Voltage regulation support along a distribution line by a virtual power plant based on a center of mass load modeling. *IEEE Trans. Smart Grid* **2018**, *9*, 3029–3038. [CrossRef]
5. Lima, R.M.; Conejo, A.J.; Langodan, S.; Hoteit, I.; Knio, O.M. Risk-averse formulations and methods for a virtual power plant. *Comput. Oper. Res.* **2018**, *96*, 350–373. [CrossRef]
6. Hooshmand, R.A.; Nosratabadi, S.M.; Gholipour, E. Event-based scheduling of industrial technical virtual power plant considering wind and market prices stochastic behaviors-A case study in Iran. *J. Clean. Prod.* **2018**, *172*, 1748–1764. [CrossRef]
7. Pasetti, M.; Rinaldi, S.; Manerba, D. A virtual power plant architecture for the demand-side management of smart prosumers. *App. Sci.* **2018**, *8*, 432. [CrossRef]
8. Li, P.; Liu, Y.; Xin, H.; Jiang, X. A robust distributed economic dispatch strategy of virtual power plant under cyber-attacks. *IEEE Trans. Ind. Inf.* **2018**, *14*, 4343–4352. [CrossRef]
9. Liu, Y.; Li, M.; Lian, H.; Tang, X.; Liu, C.; Jiang, C. Optimal dispatch of virtual power plant using interval and deterministic combined optimization. *Int. J. Electr. Power Energy Syst.* **2018**, *102*, 235–244. [CrossRef]
10. Moreno, B.; Díaz, G. The impact of virtual power plant technology composition on wholesale electricity prices: A comparative study of some European Union electricity markets. *Renew. Sustain. Energy Rev.* **2019**, *99*, 100–108. [CrossRef]
11. Kahlen, M.T.; Ketter, W.; van Dalen, J. Electric vehicle virtual power plant dilemma: Grid balancing versus customer mobility. *Prod. Oper. Manag.* **2018**, *27*, 2054–2070. [CrossRef]

12. Abdolrasol, M.G.; Hannan, M.A.; Mohamed, A.; Amiruldin, U.A.U.; Abidin, I.B.Z.; Uddin, M.N. An optimal scheduling controller for virtual power plant and microgrid integration using the binary backtracking search algorithm. *IEEE Trans. Ind. Appl.* **2018**, *54*, 2834–2844. [CrossRef]
13. Liu, Z.; Zheng, W.; Qi, F.; Wang, L.; Zou, B.; Wen, F.; Xue, Y. Optimal dispatch of a virtual power plant considering demand response and carbon trading. *Energies* **2018**, *11*, 1488. [CrossRef]
14. Di Fazio, A.R.; Russo, M.; De Santis, M. Zoning Evaluation for Voltage Optimization in Distribution Networks with Distributed Energy Resources. *Energies* **2019**, *12*, 390. [CrossRef]
15. Chen, G.; Li, J. A fully distributed ADMM-based dispatch approach for virtual power plant problems. *Appl. Math. Modell.* **2018**, *58*, 300–312. [CrossRef]
16. Di Fazio, A.R.; Russo, M.; ValeriSDeSantis, M. Linear method for steady-state analysis of radial distribution systems. *Int. J. Electr. Power Energy Syst.* **2018**, *99*, 744–755. [CrossRef]
17. Popović, Z.; Brbaklić, B.; Knežević, S. A mixed integer linear programming based approach for optimal placement of different types of automation devices in distribution networks. *Electric Power Syst. Res.* **2017**, *148*, 136–146. [CrossRef]
18. Sosnina, E.; Chivenkov, A.; Shalukho, A.; Shumskii, N. Power Flow Control in Virtual Power Plant LV Network. *Int. J. Renew. Energy Res.* **2018**, *8*, 328–335.
19. Kolenc, M.; Ihle, N.; Gutschi, C.; Nemček, P.; Breitkreuz, T.; Gödderz, K.; Zajc, M. Virtual power plant architecture using OpenADR 2.0 b for dynamic charging of automated guided vehicles. *Int. J. Electr. Power Energy Syst.* **2019**, *104*, 370–382. [CrossRef]
20. Najafi, A.; Falaghi, H.; Contreras, J.; Ramezani, M. Medium-term energy hub management subject to electricity price and wind uncertainty. *Appl. Energy* **2016**, *168*, 418–433. [CrossRef]
21. Najafi, A.; Falaghi, H.; Contreras, J.; Ramezani, M. A stochastic bilevel model for the energy hub manager problem. *IEEE Trans. Smart Grid* **2017**, *8*, 2394–2404. [CrossRef]
22. Giron, C.; Omran, S. Virtual power plant for a smart grid: A technical feasibility case study. *Int. J. Renew. Energy Res.* **2018**, *8*, 830–837.
23. Najafi, A.; Marzband, M.; Mohamadi-Ivatloo, B.; Contreras, J.; Pourakbari-Kasmaei, M.; Lehtonen, M.; Godina, R. Uncertainty-Based Models for Optimal Management of Energy Hubs Considering Demand Response. *Energies* **2019**, *12*, 1413. [CrossRef]
24. Koraki, D.; Strunz, K. Wind and solar power integration in electricity markets and distribution networks through service-centric virtual power plants. *IEEE Trans. Power Syst.* **2018**, *33*, 473–485. [CrossRef]
25. Hua, W.; Li, D.; Sun, H.; Matthews, P.; Meng, F. Stochastic environmental and economic dispatch of power systems with virtual power plant in energy and reserve markets. *Int. J. Smart Grid Clean Energy* **2018**, *7*, 231–239. [CrossRef]
26. Dall'Anese, E.; Guggilam, S.S.; Simonetto, A.; Chen, Y.C.; Dhople, S.V. Optimal regulation of virtual power plants. *IEEE Trans. Power Syst.* **2018**, *33*, 1868–1881. [CrossRef]
27. Cui, S.; Wang, Y.W.; Lin, X.; Xiao, J.W. Residential virtual power plant with photovoltaic output forecasting and demand response. *Asian J. Control.* **2019**, 1–12. [CrossRef]
28. Melchers, R.E.; Beck, A.T. *Structural Reliability Analysis and Prediction*; John Wiley&Sons: Hoboken, NJ, USA, 2018.
29. Frühwald, E.; Thelandersson, S. *Reliability Analysis*; Lund University: Lund, Sweden, 2015.
30. Hou, K.; Jia, H.; Xu, X.; Liu, Z.; Jiang, Y. A continuous time Markov chain based sequential analytical approach for composite power system reliability assessment. *IEEE Trans. Power Syst.* **2016**, *31*, 738–748. [CrossRef]
31. Najafi, A.; Farshad, M.; Falaghi, H. A new heuristic method to solve unit commitment by using a time-variant acceleration coefficients particle swarm optimization algorithm. *Turk. J. Electr. Eng. Comput. Sci.* **2016**, *23*, 354–369. [CrossRef]
32. Kennedy, J.; Eberhart, R. Particle swarm optimization (PSO). *IEEE Int. Conf. Neural Netw. Perth Aust.* **1995**, *27*, 1942–1948.